Stress hysteresis in particulate suspensions

Robert D. Deegan*
Department of Physics and Center for the Study of Complex Systems, Randall Laboratory, University of Michigan, Ann Arbor, MI 48109, USA.
(Dated: February 3, 2009)

Particulate suspensions under vibrations can support stable, localized, vertical, free-surfaces [1]. The most robust of these structures are persistent holes: deep and stable depressions of the interface. We show the existence of hysteresis in the rheological response of an aqueous suspension of cornstarch, and experimentally demonstrate how this can lead to motion that is opposite to the time-averaged applied force. A simple one-dimensional model illustrates how such motion can explain the existence of persistent holes.

The production and processing of particulate suspension is a core activity in a vast number of disparate industries from petroleum to cosmetics to consumer electronics. The most outstanding property of these materials is their propensity at high volume fractions to shear thicken [2]: their shear viscosity rises with shear rate. Despite the importance of these materials and decades of study, the physics of shear thickening remains controversial. The debate has largely pitted the order-disorder theory [3] against the hydrodynamic clustering theory [4]. Recently, Head, Adjari, & Cates introduced an alternative model, based on a mesoscopic model of the fluid [5]. Their model predicts a bistable hysteretic rheology. Here we show that particulate suspensions do indeed exhibit hysteresis in oscillatory stress tests, and furthermore demonstrate that hysteresis can give rise to dynamically stabilized states.

We begin by showing that the rheology of a shear thickening fluid undergoes a transition around a shear rate of 1 s^{-1}. We then incorporate this result into a ordinary differential equation which shows that hysteresis can give rise to time-averaged forces opposite to the applied force.

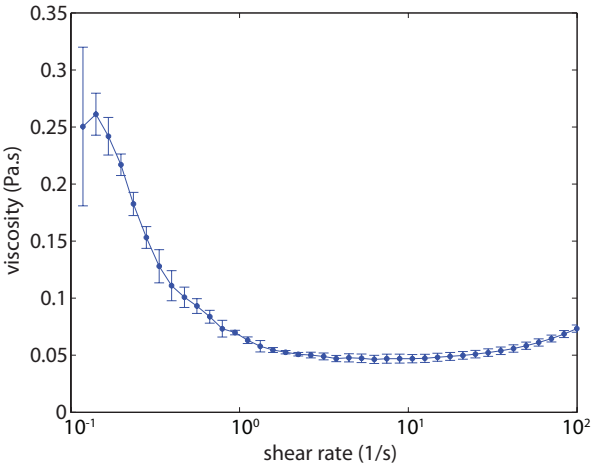

FIG. 1: Viscosity of cornstarch solution as measured in increasing shear stress ramp. The error bars correspond to the observed variation from run-to-run or sample-to-sample.

We conclude with experimental results that demonstrate the latter phenomenon.

Rheology Measurements. Our samples were prepared by mixing cornstarch (Alrich) with a 200.0 mM CsCl aqueous solution in proportions of 30%:70% by weight. The rheological properties of freshly prepared samples drifted as the sample aged, but stabilized after ∼48 hours. All measurements described below were performed after this initial aging period. A salt solution instead of pure water was used to prevent separation to due to sedimentation by density matching the granules and the solvent; no visible separation occurred in our samples over a timescale of several months. Our measurements were done on a stress controlled rheometer (AR-2000ex, TA Instruments) in a cone-plate geometry with an acrylic cone of radius $R = 3.0$ cm and angle $\alpha = 2^o$. Samples were loaded such that the normal stress never exceeded 0.1 N. Evaporation was minimized by an enclosure around the test geometry that all but sealed the test fluid from the room.

Steady-state shear viscosity measurements from shear-rate ramps exhibit the characteristic profile of particulate suspensions as shown in Fig. 1: shear thinning for low shear rates followed by shear thickening at higher shear rates. Sequential tests on the same and freshly loaded sample were reproducible to within 10%. Higher shear rates than shown in Fig. 1 produced non-rheometric flows as evidenced by the formation of waves on the meniscus and ultimately to the ejection of the fluid from the geometry.

Our primary results are from oscillatory stress tests for various stress amplitudes and frequencies. We applied a sinusoidal torque to the test fixture $\tau = \tau_o \sin 2\pi f t$ and recorded the angular displacement $\theta(t)$. For frequencies above 0.1 Hz, the combined inertia of the instrument's spindle and the test geometry is a significant factor in the motion. We subtracted this contribution from the applied stress to extract the stress on the material as follows:

$$\sigma(t) = G\left[\tau(t) - I(d^2\theta/dt^2)\right] \quad (1)$$

where G is a geometry factor for the test fixture

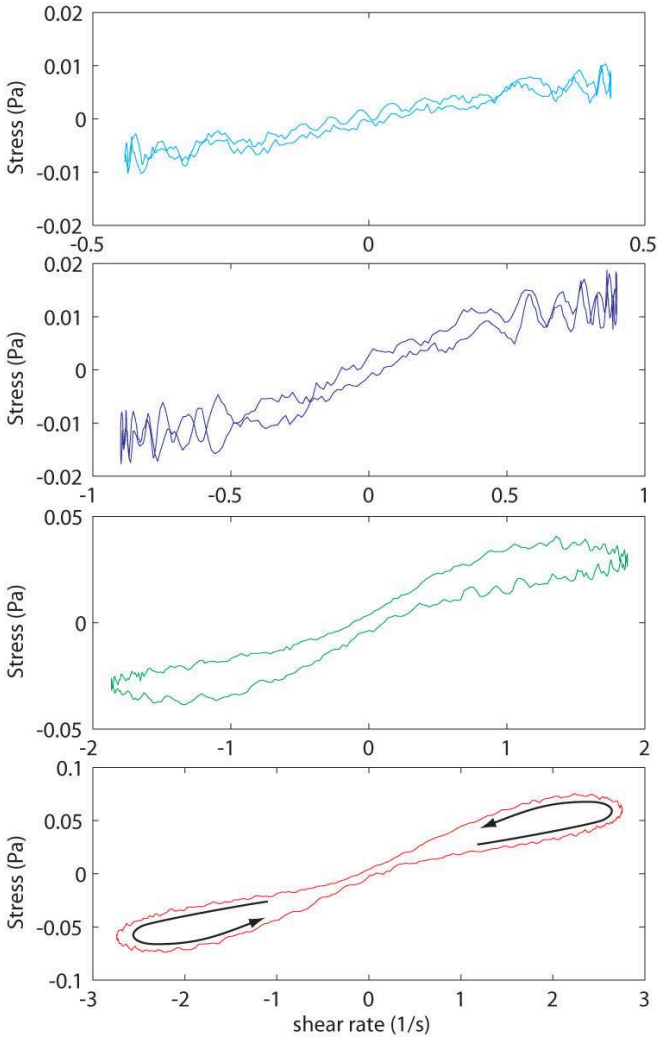

FIG. 2: Shear stress σ versus shear rate $\dot{\gamma}$ for an aqueous cornstarch mixture from oscillatory measurements at $f = 0.5$ Hz for increasing stress amplitude with low at the top. The data, as described in the text, corresponds to the instantaneous values of stress and strain rate during a single oscillation cycle. The arrows indicate increasing phase of the cycle. When the shear-rate increases beyond 1 s^{-1} the curves begin to show a hysteretic response.

$\left(\frac{2\pi R^3}{3}\right)^{-1}$, and I is the total inertia of the apparatus. The shear-rate was calculated as $\dot{\gamma} = \cot\alpha \frac{d\theta}{dt}$ where α is the cone angle.

There is only a narrow frequency and shear rate window in which quantitatively reliable data was produced. Wavelike distortions of the meniscus appeared above $\dot{\gamma} \approx 50$ s^{-1}, indicating the onset of non-rheometric flows. As the frequency of oscillation increases, the contribution of inertia to the measured torques grows as the frequency squared and ultimately dominates the signal. Extracting the material response from the signal requires twice differentiating $\theta(t)$ which introduces noise. Above 0.5 Hz the material response contribution to the torque is lost in the noise from the inertial contribution.

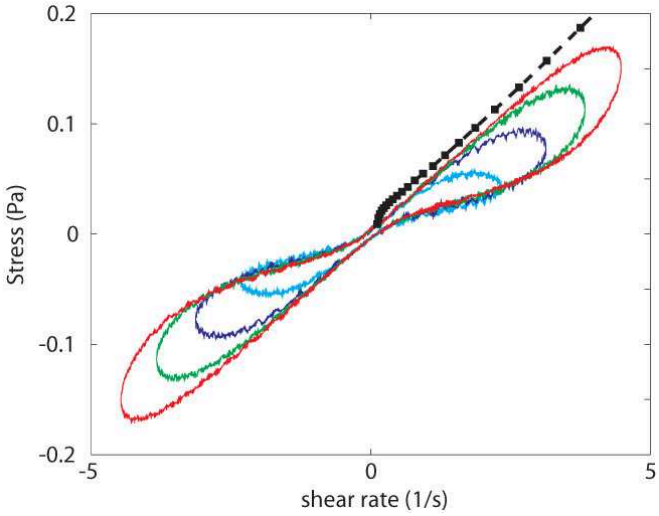

FIG. 3: Oscillatory measurements of shear stress σ versus shear rate $\dot{\gamma}$ as in Fig. 2 but for higher stresses. The black squares show the results from a steady shear measurements.

Figure 2 shows a selection of the results at $f = 0.5$ hz. These measurements were obtained by applying a low pass filter to the raw data, and averaging over 30-50 cycles. The plot shows the stress $\sigma(t)$ versus the strain rate $\dot{\gamma}$ during a single oscillation cycle. For induced shear rates less than 1 s^{-1}, these curves are essentially single valued. The small enclosed area by these curves is equivalent in magnitude to what we measure for a newtonian fluid (glycerol-water mixture) of similar viscosity. Above a shear rate of 1 s^{-1}, the stress response exhibits a qualitative change in character in which hysteresis appears. During the phases when $|\dot{\gamma}|$ is increasing, the stress is lower than during the phases when $|\dot{\gamma}|$ is decreasing. Figure 3 shows similar data to Fig. 2 but for larger torque amplitudes.

Block model of persistent holes. Merkt *et al* discovered that above an acceleration threshold a vertically vibrated suspension of non-Brownian particles supports localized structures, called persistent holes. These are approximately cylindrically symmetric depressions with a depth spanning 90% of the layer and a radial extent equal to the depth. The radius of persistent holes oscillates with the period of the drive, growing during the downward acceleration phase and shrinking during the upward phase. Persistent holes are stable despite the destabilizing action of hydrostatic pressure and surface tension which act to pull fluid into the cavity. Merkt *et al* examined various newtonian and non-newtonian fluids under similar experimental conditions, but were only able to produce persistent holes in shear thickening fluids.

We consider if the onset of hysteresis in the stress response above a stress rate threshold might explain the anomalous stability of persistent holes. We model the

behavior of persistent holes using a one degree of freedom representation for the fluid elements that comprise the walls of a persistent hole (see Fig. 4(a)). The stress on this block of fluid arises from pressure, surface tension, and stress response of the material. The pressure P is assumed to be dominated by the hydrostatic pressure; thus on the inner surface $P = P_o$ where P_o is the atmospheric pressure, and on the outer surface $P = P_o + \rho(g + a\sin\Omega t)z$ where g is the acceleration due to gravity, a and Ω are the externally applied acceleration and frequency, and ρ is the fluid density. Surface tension is neglected given the smallness of the the capillary number $\sqrt{(}\gamma/\rho a R^2) \sim 0.1$, where γ is the surface tension, and R is the size of the persistent hole. These elements yield the equation:

$$m\ddot{r} = F_P - \tilde{\sigma} \tag{2}$$

where m is the mass of the block, r is the position of the center of mass of the block, $F_P \propto (g + a\sin\Omega t)$ is the depth averaged force due to hydrostatic pressure, and $\tilde{\sigma}$ is the dissipative force that arises due to shearing of the fluid. We assume that σ depends only on the speed of the block v, is antisymmetric ($\tilde{\sigma}(\dot{r}) = -\tilde{\sigma}(-\dot{r})$) and hence independent of flow direction, and respect Le Chatelier's principle $\frac{d}{d\dot{r}}\tilde{\sigma}(\dot{r}) > 0$.

Introducing the non-dimensionalized variables $t' = \Omega t$, $v = \frac{m\Omega^2}{Cg}\dot{r}$, $\Gamma = a/g$, and $\sigma(v) = \tilde{\sigma}(\dot{r})/Cg$ yields the equation

$$\frac{dv}{dt'} = -1 + \Gamma\sin t' - \sigma(v) \tag{3}$$

Increasing r is equivalent to a growing persistent hole, and vice versa; henceforth, we say the motion is 'opening' when $r(t')$ is bigger after one cycle , and 'closing' if r is smaller.

For $\Gamma = 0$, v will monotonically approach v^* defined by $\sigma(v^*) = -1$. As $\frac{d}{dt}\tilde{\sigma}(\dot{r}) > 0$, it follows that $v^* < 0$, which corresponds to closing motion. This results is as expected for any fluid (with no yield stress), including shear thickening fluids: the free surface of a fluid will seek to restore its equilibrium configuration following a disturbance.

For $\Gamma \neq 0$ and arbitrary σ there is no analytical solution to Eq. 3. For the specific case $\sigma = \eta v$ the equation is analytically solvable and yields that the average steady-state speed $\langle v\rangle = -\eta^{-1}$. This solution corresponds to the closing type solutions expected for a Newtonian fluid.

Other likely constitutive relations were examined numerically. Models with shear thickening, with shear thinning, with shear thinning followed by shear thickening, with a yield stress, and with other discontinuities in the stress were tried. None produced opening type behavior. In all cases and for all tried parameters, $r(t')$ becomes progressively more negative, indicating that closing-type behavior is the rule for single valued constitutive models.

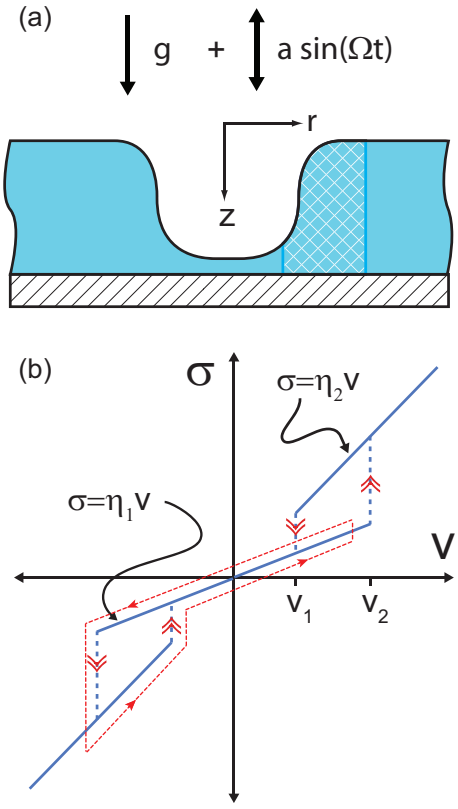

FIG. 4: (a) Schematic cross-section of persistent hole. Cross-hatched area is assumed to move as a rigid unit in the block model. Striped area is the supporting substrate. (b) Hysteretic model of viscosity. Solid horizontal lines are viscosity as a function of v. Dashed lines indicate $I \rightarrow II$ or $II \rightarrow I$ transitions when $|v|$ exceeds v_2 or falls below v_1, respectively. Dotted line shows velocity history of block during a single cycle just above acceleration threshold for opening behavior.

A hysteretic constitutive relations does produce opening solutions. To model the hysteresis observed in the rheological measurements, we set $\sigma(v) = \eta(s)v$ where s is a state variable, and η depends on s as follows:

$$\eta = \begin{cases} \eta_1 & \text{for } s = I \\ \eta_2 & \text{for } s = II \end{cases} \tag{4}$$

The state variable evolves such that s remains unchanged unless $|v|$ increases above v_2, in which case $s \rightarrow II$, or $|v|$ decreases below v_1, in which case $s \rightarrow I$. This relationship between viscosity and speed is illustrated in Fig. 4(b).

With this rheological model, Eq. 3 produces opening type solutions as well as closing type. Figure **??** show the result of a numerical integration of Eq. 3 for values which produce closing, stable and opening behavior. The physical basis of the opening solution is illustrated in Fig. 4(b). The additional forcing in the negative r direction due to gravity causes the block to reach higher speeds during the negative acceleration phase of the cycle. As the applied forcing is increased, a threshold is

passed such that the maximum speed during the negative acceleration phase surpasses the $I \rightarrow II$ transition threshold, but not during the positive phase. For this motion the effective viscosity of the system is higher during the negative phase than during the positive phase, and on average the block moves less during the former phase.

The block model predicts a counterintuitive behavior for a particle subjected to a hysteretic damping. If we apply to a particle a steady force in some particular direction, say to the right, and also apply a sinusoidal forcing, then above a threshold in the sinusoidal forcing the move particle moves to the left. The presumption thus far is that the same counterintuitive motion can manifest in a fluid. We confirmed this assumption by simultaneously applying a steady clockwise torque τ_{DC} and a sinusoidal torque τ_{AC} to the cone plate in cone-plate geometry loaded with our sample. For low values of τ_{AC}/τ_{DC}, the cone turns in the clockwise directions as expected. But above a threshold $\tau_{AC}/\tau_{DC} \simeq 20$ the cone turns counterclockwise.

We also attempted to extend the results of the block model to the continuum limit. We examined a shallow layer model in which the vertical momentum balance is assumed to be negligible. Due to the steepness of the persistent hole's walls, our assumption is not justifiable. Nonetheless, we pursued this course because the shallow layer approximation is often successful in non-shallow cases, it greatly simplifies the numerical integration of the resulting model, and is in the spirit of our approach to seek a minimal model of the persistent persistent holes in particulate suspensions. As in the single block model, the elements of fluid in the high viscosity state can initially maintain a steep surface profile. However, the high viscosity elements are surrounded by low viscosity elements which relax by diffusion and erode the high viscosity fraction. This tends to flatten the persistent hole wall and eventually the stress on the fluid, which is proportional to the surface gradient, no longer exceeds the threshold to produce hysteresis, and collapse is inevitable. In short, a shallow layer model does not support persistent holes. Further development of a continuum model should include fully 2D structures, like vortices, which were excluded from the shallow-layer model by construction but which are observed on the walls of persistent hole [1].

In summary, our study shows that particulate suspensions exhibit hysteresis. Our incorporation of a hysteretic rheology into the minimal model for persistent holes illustrates that hysteresis can generate motion opposite to the time-averaged applied stress. Our block model suggests that hysteresis can account the for the wall-like structures observed in vertically oscillations particulate suspensions [1]. This behavior, though counterintuitive, is observed in our experiments with a fluid between two plates in which a clockwise steady stress can produce counter-clockwise motion.

Our study has implications for particulate suspensions in particular and complex fluids in general. First, the existence a shear rate threshold for hysteresis in the stress response of our material suggests a microstructural transition of the fluid. While the exact nature of the mechanism responsible for shear thickening in non-Brownian suspensions is controversial (see [6, 7]), the notion of a dynamically driven structural transition is generally accepted [5, 8, 9]. Thresholds in shear [10–13], shear rate [2], and stress [14] have been alternately proposed as order parameters for this transition. Our rheology measurements are consistent with a two state system with a shear rate driven transition.

Second, our model implies that the anomalous flow found in particulate suspensions might be present in a wide range of complex fluids. We showed here that an anomalous flow can arises from hysteresis. Hysteresis is a generic feature of phase transitions, and dynamically driven microstructural transitions are common in complex fluids. Hence, we might expect similar unusual flows in complex fluids in the vicinity of microstructural transitions.

We thank Richard Kerswell for providing the shallow layer model, the Bristol Colloid Centre for use of their facility, Cheryl Flynn for assistance with the rheology measurements, Roy Hughes for discussions, and Michael Cates for helpful discussions and a critical reading of an earlier version of the manuscript.

* Electronic address: rddeegan@umich.edu

[1] F. Merkt, R. Deegan, D. Goldman, E. Rericha, and H. Swinney, Physical Review Letters **92**, 184501 (2004).
[2] H. A. Barnes, Journal of Rheology **33**, 329 (1989).
[3] R. L. Hoffman, Journal of Colloid and Interface Science **46**, 491 (1974).
[4] G. Bossis and J. F. Brady, Journal of Chemical Physics **91**, 1866 (1989).
[5] D. A. Head, A. Ajdari, and M. E. Cates, Physical Review E **64**, 061509 (2001).
[6] B. J. Maranzano and N. J. Wagner, Journal of Chemical Physics **117**, 10291 (2002).
[7] R. L. Hoffman, Journal of Rheology **42**, 111 (1998).
[8] H. M. Laun, R. Bung, and F. Schmidt, Journal of Rheology **35**, 999 (1991).
[9] O. Hess and S. Hess, Physica A **207**, 517 (1994).
[10] H. Watanabe, M. L. Yao, A. Yamagishi, K. Osaki, T. Shitata, H. Niwa, and Y. Morishima, Rheologica Acta **35**, 433 (1996).
[11] H. Watanabe, M. L. Yao, K. Osaki, T. Shikata, H. Niwa, and Y. Morishima, Rheologica Acta **36**, 524 (1997).
[12] H. Watanabe, M. L. Yao, K. Osaki, T. Shikata, H. Niwa, and Y. Morishima, Rheologica Acta **38**, 2 (1999).
[13] Y. S. Lee and N. J. Wagner, Rheologica Acta **42**, 199 (2003).
[14] J. Bender and N. J. Wagner, Journal of Rheology **40**, 899 (1996).